DOI: 10.1002/ejic.201000668

Metal Complexes of a Multidentate Cyclophosphazene with Imidazole-Containing Side Chains for Hydrolyses of Phosphoesters – Bimolecular vs. Intramolecular Dinuclear Pathway

Le Wang,[a,b] Yong Ye,[a] Vasiliki Lykourinou,[b] Alexander Angerhofer,[c] Li-June Ming,*[b] and Yufen Zhao*[a]

Keywords: Copper / Zinc / Hydrolysis / Homogeneous catalysis / Enzyme models

A multidentate imidazole-containing cyclophosphazene (Im_6Cpz) ligand was synthesized and its metal complexes (M_xIm_6Cpz; M = Zn^{II}, Cu^{II}, Co^{II}; x = 1, 2, 3) were prepared and used as phosphoesterase models towards hydrolysis of the model substrates *p*-nitrophenylphosphate (NPP) and bis(*p*-nitrophenyl)phosphate (BNPP) in 75% DMSO buffer solution at pH = 7–11 at 37 °C. The hydrolysis of BNPP by Cu_3Im_6Cpz exhibits enzyme-like saturation kinetics with $k_{cat} = 1.4 \times 10^{-5}$ s^{-1} and $k_{cat}/K_m = 0.0027$ $M^{-1}s^{-1}$. The Cu^{II} complex exhibits a tremendous selectivity toward NPP, showing nearly a stoichiometric binding with $k_{cat} = 6.8 \times 10^{-4}$ s^{-1} under saturation conditions and a significant second-order rate constant $k_{cat}/K_d = 136$ $M^{-1}s^{-1}$, which is 5.0×10^4 times higher than that for BNPP hydrolysis. An intramolecular dinuclear pathway was revealed for the complexes Cu_2Im_6Cpz and Cu_3Im_6Cpz; whereas an intermolecular dinuclear pathway was observed for $CuIm_6Cpz$. Cu_3Im_6Cpz shows an order of magnitude higher activity than the simple Cu^{II} complex of the untethered ligand *N*-methylimidazole, $Cu(MeIm)_2$, suggesting a possible contribution from the proximity effect in the Im_6Cpz complexes. The high catalytic specificity of Cu_3Im_6Cpz towards the phosphomonoester NPP suggests that it can serve as a good model system and a blueprint for further exploration of catalytic activity and specificity in phosphoester hydrolysis.

Introduction

Hydrolytic reactions promoted by mono-, di-, and multinuclear metal complexes are of increasing importance in biotechnology and medicine. Metal complex-mediated hydrolysis of phosphate esters provides valuable information for modeling and elucidating the reactivity of metal-containing nucleases as well as several dinuclear metallophosphatases involved in the cleavage of phosphoester bonds.[1] Phosphate esters and their processes exist ubiquitously in nature, such as nucleoside phosphates (nucleotides) as building blocks of RNA and DNA, sugar nucleotides for the glycosylation of oligosaccharides, and (de)phosphorylation in intracellular signaling and regulation.[2] In the absence of a catalyst or enzyme, phosphoester hydrolysis is extremely slow under normal conditions (e.g., the half life of phosphodiester hydrolysis in DNA is 3×10^7 years[3] and that of the activated phosphodiester bis(*p*-nitrophenyl)-phosphate is about 2000 years at pH 7.0 and 25 °C[4]). Moreover, with an estimated half life of an enormous 10^{11} years for the autohydrolysis of a dibasic alkylphosphate at 25 °C,[5] its hydrolysis is among the most difficult reactions catalyzed by an enzyme. Therefore, the design and synthesis of efficient and/or selective models of phosphoesterases and nucleases are regarded as a great challenge due to their value as biological tools and as chemotherapeutic agents.[6] Various di- and multinuclear metal complexes have been prepared and shown to exhibit potential cooperative effects between the metal centers.[7] Cooperative effects have been observed in multinuclear complexes of lanthanides (e.g. Ce^{IV}), Sn^{IV}, and Fe^{III} to efficiently hydrolyze the phosphodiester linkages in DNA and RNA.[8] Dinuclear Cu^{II} complexes have been reported to catalyze phosphate diester cleavage with high catalytic activities (up to 1.6×10^6 rate acceleration relative to the uncatalyzed reaction for the hydrolysis of model diester substrates at near physiological conditions).[9] Several other mono- and dinuclear complexes also show that dinuclear complexes can be superior to mononuclear complexes for hydrolysis.[10]

Cyclotriphosphazene (Cpz) comprises alternating phosphorus and nitrogen atoms with a conjugate structure to afford a planar ring. Its derivatives usually have biological miscibility and degrade into small nontoxic molecules, thus are advantageous to biological research.[11] Moreover, the rich substitution chemistry at its phosphorus centers affords the possibility for introducing other bioactive groups such as metal-binding ligands for catalyst development.[12] In

[a] Department of Chemistry, Zhengzhou University, Zhengzhou, 450052, China
E-mail: zicb@zzu.edu.cn
[b] Department of Chemistry, University of South Florida, 4202 Fowler Avenue, CHE205, Tampa, Florida 33620-5250, USA
E-mail: ming@shell.cas.usf.edu
[c] Department of Chemistry, University of Florida, Gainesville, FL 32611, USA

view of current reports and as a continuation of our previous work,[13] we derivatized Cpz with six imidazole-containing groups, (Im_6Cpz, Scheme 1) which mimic the well documented metal-binding side chain of histidine in metalloproteins. This derivative binds metal ions and mediates metal-centered hydrolysis of phosphmonoester and phosphodiester with a much higher catalytic specificity towards phosphomonoester. The mechanism has been revealed to exhibit an intramolecular dinuclear pathway when Cu:Im_6Cpz is 2:1 or 3:1. The high specificity towards phosphomonoester and the intramolecular dinuclear pathway suggest that these complexes can serve as good model systems for metallophosphatases.

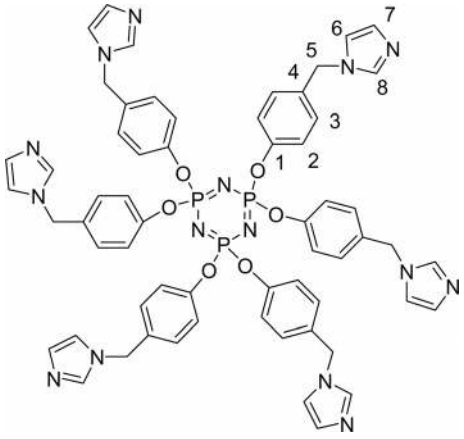

Scheme 1.

Results and Discussion

Metal binding of Im_6Cpz

Due to the existence of multiple metal binding sites in Im_6Cpz that can potentially form metal complexes with multinuclear centers, the complexes may provide mechanistic information about metal-mediated reactions, such as intermolecular vs. intramolecular and mononuclear vs. dinuclear catalytic pathways. There are two possibilities for metal binding to Im_6Cpz, "facial binding" with each metal bound to three imidazole-containing arms on each side of the Cpz ring or "extended binding" with each metal bound to two arms from the same phosphorus atom. The ^1H NMR spectra of the ligand in the presence of different amounts of Zn^{II} in [D_6]DMSO were obtained. The fluxional nature of the $Zn^{II}Im_6Cpz$ complex is attributed to chemical exchange between the Zn^{II} bound and free forms leading to gradual shift of the ^1H NMR signals of Im_6Cpz during the Zn^{II} titration. The change in the chemical shifts is plotted as a function of [Zn^{II}], which is fitted to the binding of 3 equiv. of Zn^{II} to Im_6Cpz with an apparent formation constant of $1100 \pm 730\ M^{-1}$ for Zn^{II} binding to two imidazole arms (Figure 1, A). Moreover, the addition of Cu^{II} to Im_6Cpz in DMSO/4-(2-hydroxyethyl)-1-piperazineethanesulfonic acid (HEPES) (3:1) at pH 7.1 results in a gradual increase in absorption in the region of 250–350 nm (Figure 1, B). A plot of the change in absorption at 305 nm as a function of [Cu^{II}] (Figure 1, B, inset) can be fitted to a Cu^{II}:Im_6Cpz 3:1 stoichiometry (solid trace) with a formation constant of 980 mM^{-1} for Cu^{II} binding to two imidazole arms, consistent with the stoichiometry from the NMR experiment. The weak d-d transition around 720 nm indicates a type-2 Cu^{II} center.

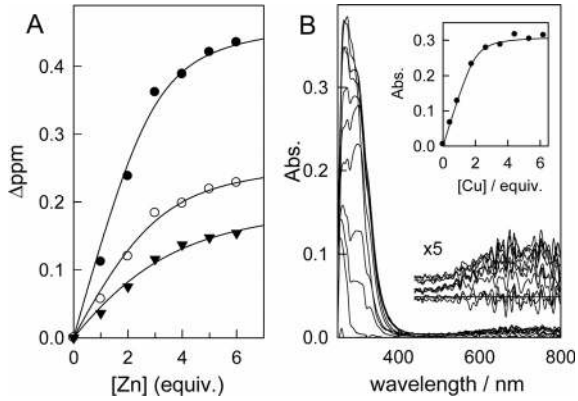

Figure 1. (A) Change of the chemical shift of the imidazole ring protons of Im_6Cpz (▼ = proton 6 at 6.928; ○ = 7 at 7.162; and ● = 8 at 7.772 ppm; Scheme 1) in [D_6]DMSO due to Zn^{II} binding; [Im_6Cpz] = 5 mM. (B) Optical titration of Cu^{II} into 0.02 mM Im_6Cpz in DMSO/HEPES 3:1 (100 mM buffer at pH 7.1) at 37 °C, monitored at 305 nm. The solid traces in (A) and (B) are the best fits to the metal:ligand 3:1 stoichiometry.

The nature of the Cu^{II} center in the complex is revealed with electron paramagnetic resonance (EPR) spectroscopy (Figure 2), in which the unpaired electron in the $d_{x^2-y^2}$ orbital of Cu^{II} affords an EPR spectrum with $g_\parallel > g_\perp$ (or $g_z > g_x$ and g_y). The EPR spectral features of the complexes with Cu:Im_6Cpz of 1:1, 2:1, and 3:1 are similar with $g_\parallel \approx 2.27$–2.30 ($A_\parallel \approx 540$–570 MHz) and $g_\perp \approx 2.07$–2.10 ($A_\perp \approx 30$–40 MHz), suggesting a similar coordination environment of the three metal centers with a nitrogen-rich coordination sphere.[14] However, the $g_\parallel$ features significantly broaden with increasing Cu^{II} binding, clearly shown in Cu_3-Im_6Cpz, suggesting the presence of a magnetic interaction possibly attributable to the proximity of the paramagnetic Cu^{II} centers.[15] The proximity of the metal centers would favor dinuclear catalysis. For spectral comparison, the all N(His) coordination sphere in Cu^{II}-substituted carbonic anhydrase B shows an electronic transition band at 750 nm and $g_\parallel = 2.31$ and $g_\perp = 2.06$[16] and Cu,Zn-superoxide dismutase exhibits a 680 nm band and $g_\parallel = 2.268$ and $g_\perp = 2.087$.[17]

Metal Binding Stoichiometry of Im_6Cpz for Catalysis

The Cu^{II} binding stoichiometry of Im_6Cpz during catalysis can be determined from Cu^{II} titration and Job plot analysis[18] by monitoring the activity towards NPP and BNPP. Detailed kinetic analyses and the mechanisms are discussed later. The activity Job plots[19] with a maximum at $X_{Cu} \approx 0.75$ are best fitted to Cu^{II}:Im_6Cpz 3:1 (i.e., X_{Cu}:X_{Im6Cpz} 0.75:0.25; Figure 3), indicating that Cu_3-Im_6Cpz is the predominant active species towards hydrolysis of NPP and BNPP and confirming that extended rather than facial binding is the preferred metal binding mode.

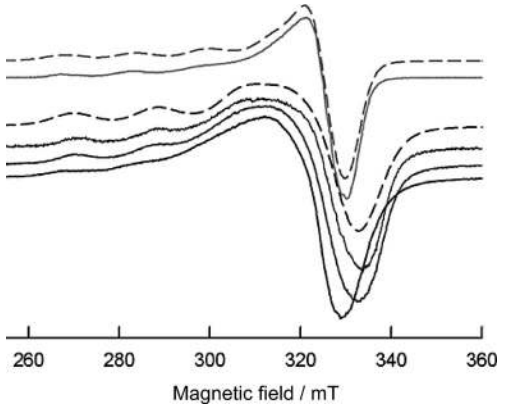

Figure 2. X-band EPR spectra of (solid traces from top to bottom at 260 mT) $Cu(MeIm)_2$ and Cu_xIm_6Cpz (x = 1, 2, 3), and simulated spectra (dashed traces) for $Cu(MeIm)_2$ ($g_\perp$ = 2.07, $g_\parallel$ = 2.318, $A_\perp$ = 18 MHz, $A_\parallel$ = 490 MHz) and $CuIm_6Cpz$ (g_x = 2.069, g_y = 2.103, g_z = 2.268, A_x = A_y = 40 MHz, A_z 573 MHz).

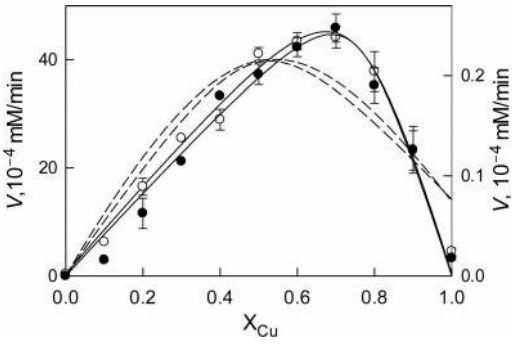

Figure 3. Activity Job plot for the determination of the stoichiometry of the Cu^{II} complex of Im_6Cpz. The total concentration of [Im_6Cpz] + [Cu^{II}] is 0.4 mM for NPP (○, left scale) and BNPP (●, right scale) hydrolysis, respectively, in 75% DMSO solution of 100 mM *N*-cyclohexyl-2-aminoethanesulfonic acid (CHES) at pH 9.0 and 37 °C. The solid traces are the best fits to the stoichiometry of Cu^{II}:ImCpz 3:1; while the dashed traces represent fits to 1:1 stoichiometry.

Phosphoester Hydrolyses by Metal Complexes of Im_6Cpz

The rate of hydrolysis of 3 mM BNPP increases with addition of Cu_3Im_6Cpz (inset, Figure 4), showing a pseudo-first order rate constant of k_{obs} = 4.5 × 10^{-6} s^{-1}. Although BNPP is considered to be quite accessible to hydrolysis due to the good leaving group *p*-nitrophenol, its hydrolytic rate is still extremely low with k_o = 1.1 × 10^{-11} s^{-1} at pH 7.0 and 25 °C,[4] which can be estimated to be 2.2 × 10^{-9} s^{-1} at pH 9.0 and 37 °C considering OH^- as the nucleophile (i.e., a 10-fold change in rate per pH unit and about two-fold rate change per 10 °C). Thus, a significant pseudo-first order rate enhancement k_{obs}/k_o = 2.0 × 10^3 can be obtained with respect to the noncatalyzed hydrolytic reaction at pH 9.0. However, since the reactions were conducted in 75% DMSO/buffer solution, the apparent ionization constant as determined by the pK_a of *p*-nitrophenol increases by 1.5 units (cf. Figure 5). Thus, the rate constant at pH 9.0 in the 75% DMSO/buffer solution is equivalent to that at pH 7.5 in buffer solution, representing a further $10^{1.5}$-fold enhancement to reach 6.3 × 10^4-fold, in aqueous solution.

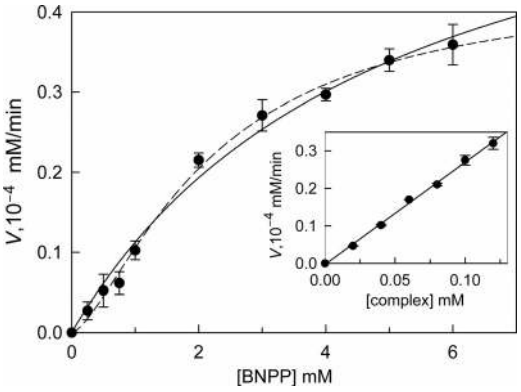

Figure 4. Plot of the initial hydrolytic rate of BNPP by 0.1 mM Cu_3Im_6Cpz fitted to Equation 2 (solid trace). The dashed traces is the fit to Hill's equation. Inset is shown the initial rate for the hydrolysis of 3 mM BNPP by different amounts of Cu_3Im_6Cpz to afford k_{obs}. Conditions: 75% DMSO in 100 mM CHES at pH 9.0 and 37 °C.

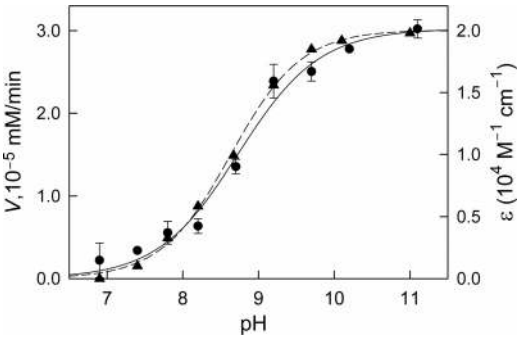

Figure 5. The pH dependence of the initial rate for the hydrolysis of 3.0 mM BNPP by Cu_3Im_6Cpz at 37 °C (● and solid fit trace) and of the molar absorptivity of *p*-nitrophenol (▲ and dashed fit trace). The molar absorptivities at different pH values were used for the determination of the reaction rates at different pH.

The rate of BNPP hydrolysis by Cu_3Im_6Cpz with respect to [BNPP] is not linear and reaches a plateau at high [BNPP] (Figure 4), indicative of pre-equilibrium kinetics analogous to enzyme catalysis [Equation (1)] with the rate law expressed as Equation (2). The data for BNPP hydrolysis can be fitted well to Equation (2) to yield the kinetic constants k_{cat} = 1.4 × 10^{-5} s^{-1} (as the first order rate constant at [S] >> K_m) and K_m = 5.2 mM, and a second order rate constant (or the catalytic efficiency) k_{cat}/K_m = 0.0027 M^{-1} s^{-1} at low [S] << K_m (Figure 4 and Table 1). Due to the change in the apparent pK_a by 1.5 units under the experimental conditions relative to that in an aqueous solution (discussed below), the rate constants are comparable to those obtained in aqueous solutions at pH 7.5 and the rate enhancements are thus 30-fold (i.e., $10^{1.5}$) higher than the values obtained from aqueous solutions at pH 9.0. A catalytic proficiency[20] of 2.0 × 10^5 is thus obtained for the

hydrolysis of BNPP in terms of first order rate constants (k_{cat}/k_o) and 1.1×10^{11} in terms of the second order catalytic efficiency[21] (k_{cat}/K_m)/k_w at pH 9.0 in 75% DMSO buffer solution, wherein $k_w = k_o/13.9$ with 13.9 M being [H_2O] in 75% aqueous DMSO solution. The kinetics for the hydrolysis of BNPP is better fitted to Hill's equation with a small Hill's coefficient $\theta = 1.5$ (dashed trace, Figure 4), suggesting the possible presence of cooperativity which may be attributable to dinuclear catalysis discussed later.

Table 1. Hydrolytic activities of M_xIm_6Cpz toward phosphoesters.[a]

Complex	k_{cat} [s^{-1}]	K_m [mM]	k_{cat}/K_m [$M^{-1}s^{-1}$]
Cu_3Im_6Cpz[b]	$(1.4 \pm 0.2) \times 10^{-5}$	5.2 ± 1.0	2.7×10^{-3}
Zn_3Im_6Cpz[b]	$(1.8 \pm 0.5) \times 10^{-6}$	1.1 ± 0.7	1.6×10^{-3}
Co_3Im_6Cpz[b]	$(6.8 \pm 0.6) \times 10^{-7}$	3.6 ± 0.7	1.9×10^{-4}
$Cu(MeIm)_2$[b]	$(2.1 \pm 0.5) \times 10^{-6}$	9.3 ± 3.1	2.3×10^{-4}
Cu_3Im_6Cpz[c]	$(6.8 \pm 0.2) \times 10^{-4}$	0.005 ± 0.001[d]	136[e]
Cu_2Im_6Cpz[c]	$(4.1 \pm 0.2) \times 10^{-4}$	0.005 ± 0.002[d]	82[e]
$CuIm_6Cpz$[c]	$(2.64 \pm 0.16) \times 10^{-4}$	0.17 ± 0.05[f]	1.6
Zn_3Im_6Cpz[c]	$(1.73 \pm 0.07) \times 10^{-4}$	0.32 ± 0.05	0.54
$Cu(MeIm)_2$[c]	$(6.1 \pm 0.4) \times 10^{-5}$	0.76 ± 0.16	8.1×10^{-2}

[a] Conditions: reaction volume = 1.0 mL in 100 mM CHES (75% DMSO) at pH = 9.0 and 37 °C, [M_xIm_6Cpz] = 0.1 mM, [BNPP] = 0.25–6.0 mM, [NPP] = 0.01–6.0 mM. [b] BNPP as the substrate. [c] NPP as the substrate. [d] Dissociation constant K_d obtained from the equilibrium: complex–NPP ⇌ complex + NPP. [e] Second-order rate constant obtained from k_{cat}/K_d. [f] The bimolecular dinuclear center is considered as a single unit in the fit to yield $K_d = 0.11 \pm 0.03$ mM.

Since metal-coordinated water molecules play a key role in metal-mediated hydrolyses, the effect of pH on BNPP hydrolysis by Cu_3Im_6Cpz was investigated. A typical sigmoidal rate–pH profile was obtained and fitted to a single proton ionization process to give pK_a = 8.73 by considering the deprotonated form as the active species (Figure 5), presumably due to a metal-bound nucleophilic OH^-. Since both Cu^{II} and Zn^{II} bind well to the ligand at pH 7.1 as shown with NMR and optical methods, the increase in rate in the rate–pH profile cannot be due to ligand ionization and metal binding but must be due to the deprotonation of the nucleophilic water. The relatively high pK_a value compared to those of many other metal complexes[29,22] reflects a low Lewis acidity of the metal center in Cu_3Im_6Cpz, which is inconsistent with the nature of the Cu^{2+} ion. Since the pK_a is significantly affected by the environment of the ionizable group, as found in the diverse environments in proteins,[23] the influence of DMSO on pK_a was addressed. The pK_a of the hydrolytic product shifts to a higher value by 1.5 units from 7.15 to 8.64 in 75% DMSO/buffer solutions. Accordingly, the pK_a value of the nucleophilic water would be ca. 7.2 in buffer solutions. A vibrational spectroscopic study indicates that DMSO elongates the ester bond, presumably by decreasing solvation on the terminal oxygen atoms;[24] however, the change in the ester bond energy is small compared to the changes in energy associated with the different reactivities of various esters. Nevertheless, electrostatic interactions are proposed to cause bond lengthening and increase in hydrolytic rate of phosphoesters. As phosphoester substrates bind to the metal center, DMSO influence on catalysis other than the pK_a is expected to be small.

Zn_3Im_6Cpz is also active towards BNPP hydrolysis ($k_{cat} = 1.8 \times 10^{-6}$ s^{-1}; Table 1), yet nearly an order lower than Cu_3Im_6Cpz. Despite its high Lewis acidity, Cu^{II} does not activate many Zn enzymes such as carboxypeptidase A and carbonic anhydrase.[25] However, a few Zn hydrolases can be significantly activated by Cu^{II} (BP10,[26] serralysin,[27] and astacin[28]). Presumably the more restricted tetragonally distorted Cu^{II} coordination relative to the flexible Zn^{II} coordination may account for the low activities in Cu^{II}-substituted Zn enzymes. In simple complexes, the coordination is more flexible relative to that in metalloenzymes which may cause Cu^{II} to exhibit high hydrolytic activities due to its higher Lewis acidity than Zn^{II}.[29] Conversely, most Co^{II}-substituted Zn hydrolases are catalytically comparable to the native enzymes, attributable to their similar coordination geometries.[25] However, Co_3Im_6Cpz shows a low activity towards BNPP hydrolysis with $k_{cat} = 6.8 \times 10^{-7}$ s^{-1} and K_m = 3.6 mM (Table 1). The smaller k_{cat} value is probably due to the relatively low Lewis acidity of the Co^{2+} ion as opposed to Co^{III} complexes with higher Lewis acidities that exhibit high k_{cat} values which, however, lacks turnover cycles due to the inertness of the Co^{3+} center.[9,30]

The k_{cat} and k_{cat}/K_m values of the complexes herein towards BNPP hydrolysis (Table 1) are higher than or comparable to several mono- and multinuclear metal complexes and metallopolymers. For example, [(1,4,7-triazacyclononane)CuOH]$^+$ exhibits $k_{obs} = 9 \times 10^{-6}$ s^{-1} at 50 °C and pH 7.2 and $k_2 = 8 \times 10^{-4}$ $M^{-1}s^{-1}$ at 35 °C;[31] Cu(bipyridine)$^{2+}$, $k_{obs} = 4.2 \times 10^{-5}$ s^{-1} at pH 6.5 and 75 °C;[32] Cu_2{N,N',N,N'-bis-[(2-hydroxybenzyl)(2-pyridylmethyl)]-2-ol-1,3-propanediamine}(μ-OAc)$(H_2O)_2Cl_2$, $k_{cat} = 5.4 \times 10^{-5}$ s^{-1} and $k_{cat}/K_m = 0.027$ $M^{-1}s^{-1}$ at pH 7.0 and 40 °C;[33] [Cu_2{*p*-6,6'-di-[bis-(2-pyridylmethyl)amino-2-methylpyridyl]benzene}$(OH)_2]^{2+}$, $k_{obs} = 1.14 \times 10^{-6}$ s^{-1} in 30% DMSO at pH 8.4 and 55 °C;[34] dinuclear [Zn_2{2,7-bis[2-(2-pyridylethyl)aminomethyl]-1,8-naphthyridine}(μ-OH)(μ-O_2Ph_2)]$^{2+}$, $k_{obs} = 6.5 \times 10^{-7}$ s^{-1} (20% acetonitrile, pH 7.0, and 40 °C);[35] a few trinuclear Zn^{II} complexes of cyclotetraamine ligands afford $(1.1–3.1) \times 10^{-4}$ $M^{-1}s^{-1}$ under various conditions;[36] and an acridine-containing di-Fe^{III} complex exhibits $k_{cat} = 5.2 \times 10^{-5}$ s^{-1} and k_{cat}/K_m = 0.017 $M^{-1}s^{-1}$ in 10% DMSO at pH 7.36 and 50 °C.[37] A chitosan-based Cu^{II} complex exhibits $k_{cat} = 8.33 \times 10^{-5}$ s^{-1} and $k_{cat}/K_m = 1.17 \times 10^{-3}$ $M^{-1}s^{-1}$ (pH 11 and 30 °C),[38] two nucleobase-containing Cu^{II} polymers show $k_{cat} = 1.13 \times 10^{-6}$ s^{-1} and $k_{cat}/K_m = 3.04 \times 10^{-5}$ $M^{-1}s^{-1}$ and 2.77×10^{-7} s^{-1} and 4.5×10^{-5} $M^{-1}s^{-1}$ (50% methanol, pH 8.0, 30 °C),[39] and the Cu^{II} complex of a pyrazolyl-Cpz-containing polymer (without a flexible linker attached to the Cpz ring) exhibits $k_{cat} = 2.93 \times 10^{-6}$ s^{-1} and $k_{cat}/K_m = 3.96 \times 10^{-3}$ $M^{-1}s^{-1}$ (50% methanol, pH 8.0, 30 °C),[40] and a metallopolymer Fe^{III}-P1, $k_{cat} = 2.2 \times 10^{-6}$ s^{-1} and $k_{cat}/K_m = 4.9 \times 10^{-3}$ $M^{-1}s^{-1}$ at pH 8.0 and 25 °C.[19b] For comparison, the catalytic specificities k_{cat}/K_m of the alternative activity

of a few enzymes toward BNPP hydrolysis are 0.05 $M^{-1} s^{-1}$ for *Escherichia coli* alkaline phosphatase,[41] 11.4 $M^{-1} s^{-1}$ for *Burkholderia* phosphonate monoester hydrolase,[42] and 0.5–100 $M^{-1} s^{-1}$ for *Streptomyces* aminopeptidase and its metal derivatives;[43] whereas a native phosphodiesterase encoded by ElaC shows a much higher value of 1480 $M^{-1} s^{-1}$.[44]

The hydrolysis of the phosphomonoester substrate NPP by Zn_3Im_6Cpz follows saturation kinetics (see ♦ in Figure 6) to afford $k_{cat} = 1.73 \times 10^{-4}$ s^{-1} and $k_{cat}/K_m = 0.54$ $M^{-1} s^{-1}$, which are 94 and 340 times, respectively, higher than those for BNPP hydrolysis (Table 1), suggesting its catalytic specificity toward phosphomonoesters. NPP hydrolysis by Cu_3Im_6Cpz also reaches a plateau at high [NPP] (see ● in Figure 6), suggesting a pre-equilibrium mechanism as in Equation (1). However, the data cannot be fitted well with Equation (2) (solid traces, Figure 6). The kinetic profile shows nearly stoichiometric NPP binding to Cu_3Im_6Cpz, indicating a very high catalytic specificity. As such, the rate law of Equation (2) is no longer valid for the mechanism in Equation (1), wherein the catalyst-bound substrate (CS) is assumed to have a lower concentration than the free form, i.e., $[S]_o >> [CS]$ to afford the term $[S]_o([E]_o - [CS])$. Thus, the steady state treatment of Equation (1) in the form of a quadratic equation $k_1([S]_o - [CS])([E]_o - [CS]) = (k_{cat} + k_{-1})[CS]$ is necessary (dashed traces; Figure 5), and affords $k_{cat} = 6.8 \times 10^{-4}$ s^{-1} under saturation conditions of $[S]_o > [Cu_3Im_6Cpz]$, a very small dissociation constant $K_d = 5$ μM for the CS complex [NPP(Cu_3Im_6Cpz)], and a significant catalytic specificity of $k_{cat}/K_d = 136$ $M^{-1} s^{-1}$ (Table 1). The k_{cat} value is 4.1×10^4 times larger than NPP autohydrolysis in 0.2 M Tris buffer at pH 9.3 ($k_o = 1.67 \times 10^{-8}$ s^{-1}).[45] This k_{cat} value is ca. 50 times higher, whereas the catalytic specificity k_{cat}/K_m is 5.0×10^4 times higher, than those for BNPP hydrolysis by Cu_3Im_6Cpz (Table 1).

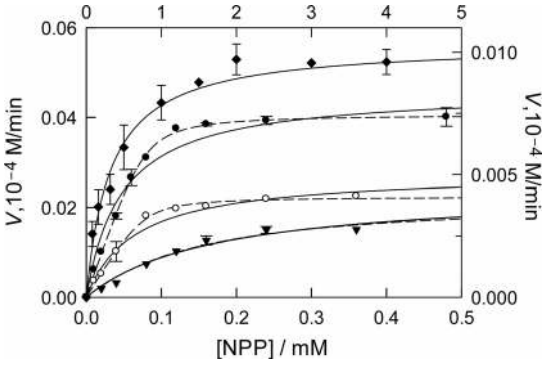

Figure 6. Plot of the initial hydrolytic rate of NPP by 0.1 mM Cu^{II} complexes (left and bottom scales) Cu_3ImCpz (●), Cu_2ImCpz (○), and $CuImCpz$ (▼) and Zn_3ImCpz (♦, top and right scales). The solid traces are fits to Equation (2) while the dashed traces are fits to a tight-binding mode. Conditions: 75% DMSO in 100 mM CHES at pH 9.0 and 37 °C.

A dinuclear Zn^{II} complex of triazacyclononane linked with a spacer shows a slightly higher hydrolytic activity toward NPP than BNPP ($k_{obs} = 2.2 \times 10^{-6}$ s^{-1} vs. 9.0×10^{-7} s^{-1})[46] and a Zn^{II} complex of a histidine mimic shows a slight preference towards NPP hydrolysis than BNPP hydrolysis at pH 7.0 and 50 °C ($k_{obs} = 2.1 \times 10^{-5}$ vs. 1.1×10^{-5} s^{-1});[47] whereas a dinuclear Cu^{II} complex exhibits a catalytic specificity toward NPP ($k_{cat} = 1.45 \times 10^{-3}$ s^{-1} and $K_m = 1.0$ mM) over BNPP (2.8×10^{-7} s^{-1})[48] and a dinuclear Cu^{II} complex of a dicyclic amine ligand shows a significantly higher catalytic specificity towards NPP than BNPP (2.2×10^{-2} vs. 9.4×10^{-4} $M^{-1} s^{-1}$).[49] However, the mononuclear Cu^{II} complex of a dicyclic amine ligand does not show such selectivity and a mononuclear Cu–cycloamine complex exhibits 500 times less activity toward NPP than BNPP,[31] suggesting the importance of a di- or multinuclear center for hydrolysis of phosphomonoesters as observed in the enzyme alkaline phosphatase.[42]

The rate constant k_{cat} for NPP hydrolysis by Cu_3Im_6Cpz was determined at different temperatures (Figure 7), from which the activation energy $E_a = 49.6$ kJ/mol was determined with the Arrhenius equation which yields the enthalpy of activation $\Delta H^{\ddagger} = 50.5$ kJ mol^{-1}. The Gibbs free energy of activation $\Delta G^{\ddagger} = 94.3$ kJ mol^{-1} was obtained from k_{cat} according to the Eyring–Polanyi equation and the entropy of activation $\Delta S^{\ddagger}$ calculated to be –144.8 J $mol^{-1} K^{-1}$. The thermodynamic parameters for the hydrolysis of NPP by Cu_2Im_6Cpz and $CuIm_6Cpz$ were also determined (E_a = 68.7 and 77.3 kJ mol^{-1}, $\Delta H^{\ddagger}$ = 65.5 and 74.5 kJ mol^{-1}, $\Delta G^{\ddagger}$ = 94.9 and 96.0 kJ mol^{-1}, and $\Delta S^{\ddagger}$ = –98.6 and –72.2 J $mol^{-1} K^{-1}$, respectively). Since the NPP hydrolysis by Cu_x-Im_6Cpz follows a pre-equilibrium kinetic pattern to form the Michaelis CS complex, the negative $\Delta S^{\ddagger}$ value reflects that the transition state $CS^{\ddagger}$ is much better organized than the CS complex. The hydrolysis of bound NPP in the inert complex *cis*-[Co(en)$_2$(OH)(NPP)], which mimics the Michaelis CS complex, has $\Delta S^{\ddagger} = -65$ J $mol^{-1} K^{-1}$,[50] close to that for NPP hydrolysis by $CuIm_6Cpz$. Conversely, NPP autohydrolysis showed $\Delta S^{\ddagger} = -18.8$ J $mol^{-1} K^{-1}$ and was suggested to follow a dissociative mechanism[51] which nevertheless was questioned.[52] Crystallographic "snapshots" of phosphoserine phosphatase with a bound substrate (D11N mutant), transition state analogues, and the phosphate product [53] revealed that the transition state analogues in

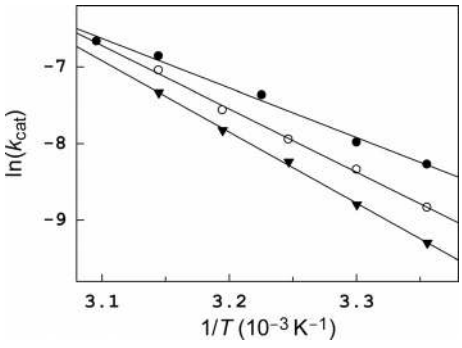

Figure 7. Temperature dependence of k_{cat} for the hydrolysis of NPP by Cu_3Im_6Cpz (●), Cu_2Im_6Cpz (○), and $CuIm_6Cpz$ (▼) in 75% DMSO of 100 mM CHES at pH 9.0. The activation energy E_a is obtained by directly fitting to the Arrhenius equation.

the enzyme showed the reaction coordinate distances of 3.59 and 3.56 Å which are significantly shorter than the distance of 4.9 Å estimated for the fully dissociative mechanism, suggesting an associative mechanism.

Mechanistic Investigation

Because Im_6Cpz is capable of binding up to three equivalents of metal, it is therefore important to gain further insight into possible interactions among the three metal centers in substrate binding and hydrolytic activity. The kinetic traces for hydrolysis of BNPP and NPP can be better fitted by the use of Hill's equation with Hill's coefficients $\theta = 1.47$ and 1.42, respectively, indicative of cooperativity and a dinuclear pathway. The charged $>PO_2^-$ moiety in BNPP and NPP is feasible for interaction with two metal centers to render a dinuclear pathway.

The (MIm_6Cpz):S ratio in the pre-equilibrium $MIm_6Cpz + S \rightleftharpoons (MIm_6Cpz)$–S can be determined by means of the mechanistic Job plot[19] using hydrolytic activity (which is proportional to [(MIm_6Cpz)–S]; Equation (1)) instead of optical density as the output. The maximum in the mechanistic Job plot thus reflects the (MIm_6Cpz):S ratio in the catalysis. The data show a maximum at $X_{complex}$ ca. 0.5 for NPP hydrolysis by Cu_2Im_6Cpz and Cu_3Im_6Cpz which can be best fitted with (Cu_xIm_6Cpz):NPP = 1:1 (Figure 8), i.e., $X_{complex}$:X_{NPP} = 0.5:0.5. In the case of Cu_2Im_6Cpz, the 1:1 ratio may suggest an intermediate (Cu_2Im_6Cpz)–NPP with an internal dinuclear center formed by two Cu bound arms or ($Cu_2Im_6Cpz)_2$–NPP_2 with two dinuclear centers formed by two metal complexes (which is thermodynamically unfavorable). In the case of Cu_3Im_6Cpz, the substrates may bind to an intramolecular dinuclear metal center as in (Cu_2Im_6Cpz)–NPP, which would leave one mononuclear arm. The higher activity of Cu_3Im_6Cpz than Cu_2Im_6Cpz (Table 1) may be due to a higher probability of collision attributable to the three metal centers, or because all the three metal centers are active.

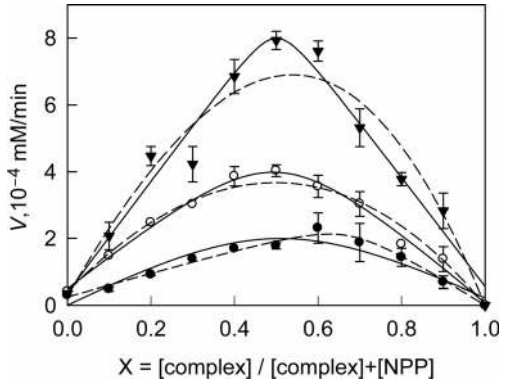

Figure 8. Mechanistic Job plot of Cu_3Im_6Cpz (▼), Cu_2Im_6Cpz (○), and $CuIm_6Cpz$ (●) towards the hydrolysis of NPP with a constant total concentration ([complex] + [NPP]) of 0.1 mM (25 °C, pH = 9.0 75% DMSO). The data are fitted to the stoichiometry of complex:NPP = 1:1 (solid traces) or 2:1 (dashed traces).

Owing to the very low solubility of the metal complexes, attempts to grow crystals were unsuccessful. Possible arrangement of the six arms of Im_6Cpz upon metal binding was modeled with geometry-optimized molecular mechanics calculations, which shows that two metal centers can be in close proximity with a possible OH^-/O^{2-} bridging ligand and a pseudo-twofold symmetry of the two arms (Figure 9). Such an arrangement suggests a probable intramolecular dinuclear catalytic pathway. Although such a dinuclear center during catalysis does not need to be present in the resting state of the complexes, the gradual increase in broadness of the EPR spectra with increasing amount of Cu^{II} in the complex suggests the presence of magnetic interactions due to the proximity of the Cu^{II} centers.

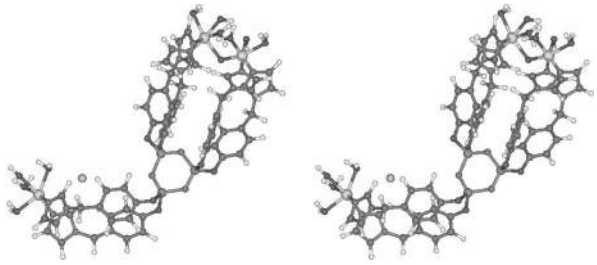

Figure 9. A plausible structure of the Cu_3Im_6Cpz complex with an intramolecular dinuclear center obtained from molecular mechanics calculations (BioMedCAChe 6.1, Fujitsu). One coordinated water on each Cu^{II} center is assigned as the deprotonated OH^- and the dinuclear site is bridged by an oxide. A Cl^- ion was added as a counterion to balance the charge.

The kinetic pattern of NPP hydrolysis by $CuIm_6Cpz$ is significantly different from those by Cu_2Im_6Cpz and Cu_3Im_6Cpz (Figure 6), suggesting different catalytic mechanisms. For example, $CuIm_6Cpz$ would not be likely to form an intramolecular dinuclear center as Cu_2Im_6Cpz and Cu_3Im_6Cpz do. The mechanistic Job plot for NPP hydrolysis by $CuIm_6Cpz$ shows a maximum at $X_{complex}$ ca. 0.65, which can be fitted with a $CuIm_6Cpz$:NPP ratio of 2:1 (● and dashed trace; Figure 8), i.e., $X_{complex}/X_{NPP}$ ca. 0.65:0.35, suggesting a dinuclear center formed by two complex molecules. Accordingly, Cu_3Im_6Cpz can form an intramolecular dinuclear center as in Cu_2Im_6Cpz and an intermolecular dinuclear center as in $CuIm_6Cpz$ for two parallel pathways during hydrolytic catalysis of NPP. In such a case, the Cu_3Im_6Cpz:NPP ratio would be 2:3, which is thermodynamically less favorable. The active intermediate during Cu_3Im_6Cpz catalysis is likely to be NPP–(Cu_3Im_6Cpz)–NPP–(Cu_3Im_6Cpz) or to simply follow both intra- and intermolecular dinuclear pathways. Indeed, the k_{cat} value of Cu_3Im_6Cpz ($6.8 \times 10^{-4}\,s^{-1}$) is the sum of those of Cu_2Im_6Cpz ($4.1 \times 10^{-4}\,s^{-1}$) following an intramolecular pathway and $CuIm_6Cpz$ ($2.64 \times 10^{-4}\,s^{-1}$) following an intermolecular pathway.

$Cu(MeIm)_2$

The mechanism of the Cu_xIm_6Cpz complexes are further investigated with a simple mimetic system, the Cu^{II} complex with MeIm which represents a metal center not tethered to the Cpz core. The binding of MeIm to Cu^{II} is demonstrated by an electronic transition at 700 nm which reaches a plateau at the addition of 2 equiv. of MeIm, indicative of the formation of the complex $Cu(MeIm)_2$ in solution (Fig-

ure 10, A). $Cu(MeIm)_2$ exhibits an EPR spectrum with $g_{\|}$ = 2.318, $A_{\|}$ = 490 MHz, $g_{\perp}$ = 2.074, and $A_{\perp}$ = 18 MHz (Figure 2). Addition of more MeIm results in a slight shift of the electronic transition to 670 nm (inset, Figure 10, A), suggesting the formation of a different complex. For comparison, the hydrolytic activities of $Cu(MeIm)_2$ towards BNPP and NPP were determined under the same conditions as for Cu_3Im_6Cpz (Figure 10, B), showing k_{cat} values up to two orders of magnitude smaller than Cu_3Im_6Cpz and K_m values about an order higher (Table 1). As $K_m = (k_{cat} + k_{-1})/k_1$, a large decrease in k_{cat} and a significant increase in K_m reflect a large increase in the dissociation of the catalyst–substrate complex (or poor substrate binding). This observation demonstrates that Cu_3Im_6Cpz is superior to the simple complex $Cu(MeIm)_2$ in terms of substrate recognition and hydrolytic catalysis. The stoichiometry of the $[Cu(MeIm)_2]$–NPP intermediate was also determined with the mechanistic Job plot. The data were better fitted to the stoichiometry of $Cu(MeIm)_2$:NPP = 2:1 (Figure 10, C), representing a intermolecular dinuclear pathway as found in the case of $CuIm_6Cpz$ catalysis.

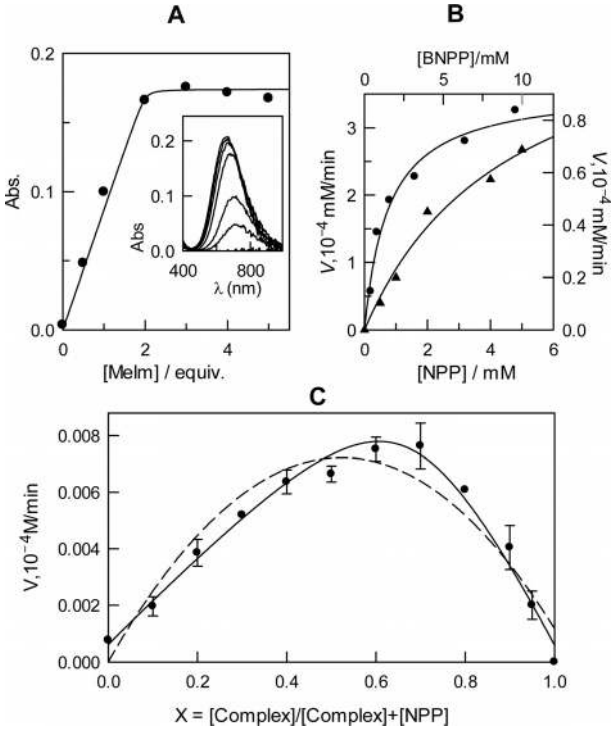

Figure 10. (A) Optical titration of MeIm into 4 mM Cu^{II} in methanol at 37 °C, monitored at 700 nm. The solid trace is the fitting to the formation of a 1:2 (ML_2) complex. (B) Hydrolysis of BNPP (▲; right scale) and NPP (●; left scale) by $Cu(MeIm)_2$. (C) A mechanistic job plot of NPP hydrolysis by $Cu(MeIm)_2$ with [complex] + [NPP] = 1.0 mM. The data are fitted to $Cu(MeIm)_2$:NPP 2:1 (solid trace) and 1:1 (dashed trace). Conditions: 75% DMSO in 100 mM CHES at pH 9.0 and 37 °C.

Conclusion

A Cpz core functionalized with six imidazole-containing arms has been shown to bind up to three divalent metal ions. The resulting complexes can effectively catalyze the hydrolysis of the phosphomonoester NPP and phosphodiester BNPP in 75% DMSO in buffer, with a tremendous selectivity towards NPP over BNPP by 5.0×10^4 times in terms of catalytic specificity k_{cat}/K_m for Cu_3Im_6Cpz. Compared with an untethered imidazole complex of Cu^{II}, Cu_2Im_6Cpz and Cu_3Im_6Cpz exhibit up to two-order higher rates toward phosphoester hydrolysis in terms of k_{cat}, suggesting that the proximity of metal centers in these complexes are catalytically significant analogous to the multinuclear center in alkaline phosphatase. The catalysis follows an *intramolecular* pathway with the substrate NPP bound to two Cu^{II} centers in Cu_2Im_6Cpz and Cu_3Im_6Cpz, but an *intermolecular* pathway in $CuIm_6Cpz$ with the substrate bound to two complexes in which the intramolecular pathway is not available. These complexes display significant catalytic proficiencies and unique catalytic mechanism and can also serve as new structural motifs for further exploration of chemical modeling.

Experimental Section

Materials: Im_6Cpz was synthesized following a previously established method.[13] All reagents are commercially available, solvents distilled and dried with standard procedures, and aqueous solutions prepared from 18 MΩ deionized or distilled water. The 75% DMSO buffer solutions were prepared by direct mixing DMSO with the buffer at a desired pH, HEPES (pH 7.0–8.0) and CHES (pH 9–10.0) at 100 mM. The pK_a value (7.15) of the hydrolytic product *p*-nitrophenol changes with the addition of DMSO and becomes 8.64 in the presence of 75% DMSO, which affect its molar absorptivity at different pHs and are calibrated based on the fully deprotonated form.

Spectroscopic and Kinetic Measurements: NMR spectra were recorded with a Varian INOVA500 spectrometer. Electronic spectra and all kinetic measurements were performed with a Varian Cary 50 spectrophotometer. EPR spectra were obtained with a Bruker Elexsys E580 X-band spectrometer at ca. 5–6 K using an Oxford ESR900 cryostat and the Bruker standard rectangular TE_{102} resonator, typically with a microwave frequency ca. 9.4 GHz, field modulation around 2 G, and time constant/conversion time settings of 40/80 ms. The *g* and *A* values were obtained from spectral simulations performed with the "easyspin" toolbox for Matlab.[54]

The initial rates of the hydrolysis of all the phosphoester substrates were monitored spectrophotometrically between 10 and 60 min through the change at 419 nm due to the production of *p*-nitrophenolate (measured in 75% DMSO/buffer of 100 mM at 37 °C, ε = 15,600 $M^{-1}cm^{-1}$ at pH 9.0). Various amounts of the complex and substrates were used in the reactions separately, from which the rate laws were determined and the rate constants obtained by means of nonlinear regression. The kinetics can be described as the binding of the substrate S to the metal center to form an intermediate S–$[Cu_3Im_6Cpz]$ complex, followed by conversion to the products; see Equation (1). The pre-equilibrium rate law is expressed as Equation (2) with the assumption that the amount of bound S is much less than that of free S in solution, in which $K_m = (k_{-1} + k_{cat})/k_1$ is the virtual dissociation constant of the bound S, equivalent to the Michaelis constant in enzyme catalysis.

$$Cu_3\text{–}Im_6Cpz + S \underset{k_{-1}}{\overset{k_1}{\rightleftharpoons}} S\text{–}(Cu_3\text{–}Im_6Cpz) \xrightarrow{k_{cat}} Cu_3\text{–}Im_6Cpz + P \quad (1)$$

$$\text{Rate} = k_{cat}\,[Cu_3ImCpz][S] / (K_m + [S]) \quad (2)$$

In the optical Job plots, the total concentration of the metal plus the ligand is kept constant while varying the metal:ligand ratio and monitored by the optical density of the complex. The formation of the S–(metal complex) ternary complex is under equilibrium, thus the stoichiometry of the ternary complex can be determined by the Job plot method,[18] but monitored by the activity rather than the optical density of the ternary complex.[19] In the case of the activity Job plot, the total concentration of the metal complex and S is kept constant by varying the complex:S ratio and monitoring the hydrolytic activity.[19]

Computer Modeling: Molecular mechanics calculations of the metal binding mode using the MM3 protocol[55] were performed by the use of BioMedCAChe version 6.1.10 (Fujitsu, Beaverton, Oregon). The coordination geometry of the metal is set to octahedral, and the metal is considered to bind to the imidazole on the side arms in plane with the imidazole ring. Any distortion from this coordination geometry is not considered to be a favorable metal binding mode.

Acknowledgments

We are grateful for financial support from the National Natural Science Foundation of China (grant numbers 20602032, 20732004, 20972143). The research on catalyses by "Nature's Minimalistic Systems" sponsored by the National Science Foundation of U.S.A. (LJM, CHE-0718625) is also acknowledged. Work at the University of Florida was supported by the National Science Foundation of U.S.A. (CHE-0809725, to A. A.).

[1] a) R. Ott, R. Krämer, *Appl. Microbiol. Biotechnol.* **1998**, *52*, 761–767; b) J. A. Cowan, *Curr. Opin. Chem. Biol.* **2001**, *5*, 634–642; c) A. Sreedhara, J. A. Cowan, *J. Biol. Inorg. Chem.* **2001**, *6*, 337–347; d) S. J. Franklin, *Curr. Opin. Chem. Biol.* **2001**, *5*, 201–208; e) M. Komiyama, J. Sumaoka, *Curr. Opin. Chem. Biol.* **1998**, *2*, 751–757; f) L. R. Gahan, S. J. Smith, A. Neves, G. Schenk, *Eur. J. Inorg. Chem.* **2009**, 2745–2758.

[2] S. Aoki, E. Kimura, *Rev. Mol. Biol.* **2002**, *90*, 129–155.

[3] G. K. Schroeder, C. Lad, P. Wyman, N. H. Williams, R. Wolfenden, *Proc. Natl. Acad. Sci. USA* **2006**, *103*, 4052–4055.

[4] a) J. Chin, M. Banaszczyk, Y. Zubian, X. Zou, *J. Am. Chem. Soc.* **1989**, *111*, 186–190; b) B. K. Takasaki, J. Chin, *J. Am. Chem. Soc.* **1995**, *117*, 8582–8585.

[5] C. Lad, N. H. Williams, R. Wolfenden, *Proc. Natl. Acad. Sci. USA* **2003**, *100*, 5607–5610.

[6] a) J. D. Sreedhara, J. A. Freed, J. A. Cowan, *J. Am. Chem. Soc.* **2000**, *122*, 8814–8824; b) F. Manicin, P. Scrimin, P. Tecilla, U. Tonellato, *Chem. Commun.* **2005**, 2540–2548; c) D. S. Sigman, *Biochemistry* **1990**, *29*, 9097–9105; d) P. U. Maheswari, S. Roy, H. Dendulk, S. Barends, G. V. Wezel, J. Reedijk, *J. Am. Chem. Soc.* **2006**, *128*, 710–711.

[7] a) S. T. Frey, H. J. Sun, N. N. Murphy, K. D. Karlin, *Inorg. Chim. Acta* **1996**, *242*, 329–331; b) A. Neves, H. Terenzi, R. Horner, A. Horn, B. Szpoganicz, J. Sugai, *Inorg. Chem. Commun.* **2001**, *4*, 388–391; c) C. Liu, M. Wang, T. Zhang, H. Sun, *Coord. Chem. Rev.* **2004**, *248*, 147–168; d) A. K. Yatsimirsky, *Coord. Chem. Rev.* **2005**, *249*, 1997–2011; e) X. D. Dong, X. Y. Wang, M. X. Lin, H. Sun, X. L. Yang, Z. J. Guo, *Coord. Chem. Rev.* **2007**, *251*, 1951–1972.

[8] a) M. Irisawa, M. Komiyama, *J. Biochem.* **1995**, *117*, 465–466; b) M. Komiyama, N. Takeda, H. Shigekawa, *Chem. Commun.* **1999**, 1443–1451; c) N. Takeda, M. Shibata, N. Tajima, K. Hirao, M. Komiyama, *J. Org. Chem.* **2000**, *65*, 4391–4396.

[9] a) N. H. Williams, B. Takasaki, M. Wall, *J. Chin. Acc. Chem. Res.* **1999**, *32*, 475–484; b) J. Chin, *Curr. Opin. Chem. Biol.* **1997**, *1*, 514–521; c) J. R. Morrow, O. Iranzo, *Curr. Opin. Chem. Biol.* **2004**, *8*, 192–200.

[10] a) Y. Hang, H. H. Lin, X. Q. Yu, *Bioorg. Med. Chem.* **2008**, *16*, 1103–1110; b) Y. G. Fang, J. Zhang, S. Y. Chen, N. Jiang, Y. Zhang, X. Q. Yu, *J. Bioorg. Med. Chem.* **2007**, *15*, 696–701; c) Q. L. Li, J. Huang, Q. Wang, X. Q. Yu, *J. Bioorg. Med. Chem.* **2006**, *14*, 4151–4157; d) K. Selmeczi, M. Giorgi, G. Speier, E. Farkas, M. Reglier, *Eur. J. Inorg. Chem.* **2006**, 1022–1031.

[11] a) H. R. Allcock, *Science* **1976**, *193*, 1214–1219; b) H. R. Allcock, *Chemistry and Applications of Polyphosphazenes*, Wiley Interscience, Hoboken, NJ, **2003**.

[12] a) P. Pertici, G. Vitulli, P. Salvadori, E. Pitzalis, M. Gleria, *Phosphazenes* **2004**, 621–631; b) V. Chandrasekhar, A. Athimoolam, S. G. Srivatsan, P. S. Shanmuga, S. Verma, A. Steiner, S. Zacchini, R. Butcher, *Inorg. Chem.* **2002**, *41*, 5162–5173.

[13] a) L. Wang, Y. Ye, Y. F. Zhao, *Chin. Chem. Lett.* **2009**, *20*, 58–61; b) M. Y. Niu, Y. Ye, W. Liu, *Chem. J. Chin. Univ.* **2006**, *27*, 1253–1255; c) Y. F. Zhao, X. H. Li, Y. Ma, *China's Patent No*: ZL 961 14313 4, **1996**; d) Y. S. Li, Y. F. Zhao, Y. Wan, *J. Bioorg. Med. Chem.* **2000**, *8*, 2675–2678.

[14] J. Peisach, W. E. Blumberg, *Arch. Biochem. Biophys.* **1974**, *165*, 691–708.

[15] V. Lykourinou, A. I. Hanafy, G. F. Z. da Silva, K. S. Bisht, R. W. Larsen, B. T. Livingston, A. Angerhofer, L.-J. Ming, *Eur. J. Inorg. Chem.* **2008**, 2584–2592.

[16] I. Bertini, E. Borghi, C. Luchinat, *J. Am. Chem. Soc.* **1979**, *101*, 7069–7071.

[17] a) R. J. Carrico, H. F. Deutsch, *J. Biol. Chem.* **1969**, *244*, 6087–6093; b) G. Rotilio, A. F. Agro, L. Calabrese, F. Bossa, P. Guerrieri, B. Mondovi, *Biochemistry* **1971**, *10*, 616–621.

[18] C. Y. Huang, *Meth. Enzymol.* **1982**, *87*, 509–525.

[19] a) W. M. Tay, J. D. Epperson, G. F. Z. da Silva, L.-J. Ming, *J. Am. Chem. Soc.* **2010**, *132*, 5652–5661; b) V. Lykourinou, A. I. Hanafy, K. S. Bisht, A. Angerhofer, L.-J. Ming, *Eur. J. Inorg. Chem.* **2009**, 1199–1207.

[20] a) A. Radzicka, R. Wolfenden, *Science* **1995**, *267*, 90–93; b) D. B. Northrop, *Adv. Enzymol. Relat. Areas Mol. Biol.* **1999**, *73*, 25–55.

[21] P. J. OBrien, D. Herschlag, *J. Am. Chem. Soc.* **1998**, *120*, 12369–12370.

[22] a) E. Kimura, T. Koike, *Adv. Inorg. Chem.* **1997**, *44*, 229–261; b) E. Kimura, *Prog. Inorg. Chem.* **1994**, *41*, 443–491; c) N. H. Williams, B. Takasaki, M. Wall, *J. Chin,. Acc. Chem. Res.* **1999**, *32*, 485–493; d) A. Blasko, T. C. Bruice, *Acc. Chem. Res.* **1999**, *32*, 475–484; e) H. Vahrenkamp, *Acc. Chem. Res.* **1999**, *32*, 589–596; f) R. Ott, R. Kramer, *Appl. Microbiol. Biochem.* **1999**, *52*, 761–767.

[23] a) F. Milletti, L. Storchi, G. Cruciani, *Prot. Struct., Funct., Bioinform.* **2009**, *76*, 484–495; b) P. Barth, T. Alber, P. B. Harbury, *Proc. Natl. Acad. Sci. USA* **2007**, *104*, 4898–4903.

[24] H. Cheng, I. Nikolic-Hughes, J. H. Wang, H. Deng, P. J. O'Brien, L. Wu, Z.-Y. Zhang, D. Herschlag, R. Callender, *J. Am. Chem. Soc.* **2002**, *124*, 11295–11306.

[25] I. Bertini, C. Luchinat, in: *Bioinorganic Chemistry* (Eds.: I. Bertini, H. B. Gray, S. J. Lippard, J. S. Valentine), University Science Books, CA, chapter *2*, **1994**.

[26] G. F. Z. da Silva, R. L. Reuille, L.-J. Ming, B. T. Livingston, *J. Biol. Chem.* **2006**, *281*, 10737–10744.

[27] H. I. Park, L.-J. Ming, *J. Biol. Inorg. Chem.* **2002**, *7*, 600–610.

[28] a) F. X. Gomis-Rüth, F. Grams, I. Yiallouros, H. Nar, U. Küsthardt, R. Zwilling, W. Bode, W. Stöcker, *J. Biol. Chem.*

1994, *269*, 17111–17117; b) H. I. Park, L.-J. Ming, *J. Inorg. Biochem.* **1998**, *72*, 57–62.
[29] E. L. Hegg, J. N. Burstyn, *Coord. Chem. Rev.* **1998**, *173*, 133–165.
[30] J. Chin, M. Banaszczyk, V. Jubian, X. Zou, *J. Am. Chem. Soc.* **1989**, *111*, 186–190.
[31] E. L. Hegg, S. H. Mortimore, C. Cheung, J. E. Huyett, D. R. Powel, J. N. Burstyn, *Inorg. Chem.* **1999**, *38*, 2792–2798.
[32] J. R. Morrow, W. C. Trogler, *Inorg. Chem.* **1988**, *27*, 3387–3394.
[33] L. M. Rossi, A. Neves, R. Horner, H. Terenzi, B. Szpoganicz, J. Sugai, *Inorg. Chim. Acta* **2002**, *337*, 366–370.
[34] L. Zhu, O. dos Santos, C. W. Koo, M. Rybstein, L. Pape, J. W. Canary, *Inorg. Chem.* **2003**, *42*, 7912–7920.
[35] N. V. Kaminskaia, C. He, S. J. Lippard, *Inorg. Chem.* **2000**, *39*, 3365–3373.
[36] C. Bazzicalupi, A. Bencini, E. Berni, C. Giorgi, S. Maoggi, B. Valtancoli, *Dalton Trans.* **2003**, 3574–3580.
[37] X. Q. Chen, X. J. Peng, J. Y. Wang, Y. Wang, S. Wu, L. Z. Zhang, T. Wu, Y. K. Wu, *Eur. J. Inorg. Chem.* **2007**, 5400–5407.
[38] Y.-C. Chang, D.-H. Chen, *React. Funct. Polym.* **2009**, *6*, 601–605.
[39] S. G. Srivatsan, S. Verma, *Chem. Eur. J.* **2001**, *7*, 828–833.
[40] V. Chandrasekhar, A. Athimoolam, S. G. Srivatsan, P. S. Sundaram, S. Verma, A. Steiner, S. Zacchini, R. Butcher, *Inorg. Chem.* **2002**, *41*, 5162–5173.
[41] D. Herschlag, P. J. O'Brien, *Biochemistry* **2001**, *40*, 5691–5699.
[42] S. B. Dotson, C. E. Smith, C. S. Ling, G. F. Barry, G. M. Kishore, *J. Biol. Chem.* **1996**, *271*, 25754–25761.
[43] a) H. I. Park, L.-J. Ming, *Angew. Chem. Int. Ed.* **1999**, *38*, 2914–2916; b) A. Ercan, H. I. Park, L.-J. Ming, *Chem. Commun.* **2000**, 2501–2502; c) A. Ercan, H. I. Park, L.-J. Ming, *Biochemistry* **2006**, *45*, 13779–13793; d) A. Ercan, W. M. Tay, S. H. Grossman, L.-J. Ming, *J. Inorg. Biochem.* **2010**, *104*, 19–29.
[44] A. Vogel, O. Schilling, M. Niecke, J. Bettmer, W. Meyer-Klaucke, *J. Biol. Chem.* **2002**, *277*, 29078–29085.
[45] A. J. Kirby, W. P. Jencks, *J. Am. Chem. Soc.* **1965**, *87*, 3209–3216.
[46] W. H. Chapman, R. Breslow, *J. Am. Chem. Soc.* **1995**, *117*, 5462–5469.
[47] K. Ichikawa, M. Tarnai, M. K. Uddin, K. Nakata, S. Sato, *J. Inorg. Biochem.* **2002**, *91*, 437–450.
[48] A. Jancso, I. Torok, K. Hegetschweiler, T. Gajda, *ARKIVOC* **2009**, *3*, 217–224.
[49] J. H. Kim, *Chem. Lett.* **2000**, 156–157.
[50] D. R. Jones, L. F. Lindoy, A. M. Sargeson, *J. Am. Chem. Soc.* **1983**, *105*, 1321–1336.
[51] A. J. Kirby, A. G. Varvoglis, *J. Am. Chem. Soc.* **1967**, *89*, 415–423.
[52] J. Åqvist, K. Kolmodin, J. Florian, A. Warshel, *Chem. Biol.* **1999**, *6*, R71–R80.
[53] W. R. Wang, H. S. Cho, R. Kim, J. Jancarik, H. Yokota, H. H. Nguyen, I. V. Grigoriev, D. E. Wemmer, S. H. Kim, *J. Mol. Biol.* **2002**, *319*, 421–431.
[54] S. Stoll, A. Schweiger, *J. Magn. Reson.* **2006**, *178*, 42–55.
[55] N. L. Allinger, Y. H. Yuh, J. H. Lii, *J. Am. Chem. Soc.* **1989**, *111*, 8551–8566.

Received: June 18, 2010
Published Online: January 3, 2011

